



### RESEARCH ARTICLE

#### Reactional impact of nickel sulphate hydrate on the hydrolysis for different oil shale layers from the Tarfaya deposit (Morocco)

Abdeljabbar Attaoui

Department of Chemistry, Faculty of Sciences Ben m'sik Casablanca, University Hassan II (Morocco).

#### Manuscript Info

##### Manuscript History

Received: 05 December 2023

Final Accepted: 09 January 2024

Published: February 2024

#### Abstract

Nickel catalysis has been studied for coal tars and graphite carbon to produce CH<sub>4</sub> methane in the presence of hydrogen. Nickel forms mixed complexes with the  $\gamma$  and  $\beta$ pycoline (P.F. Neson: 1988). In this work, we have focused on the mineral part formed mainly by calcite, dolomite, pyrite and other mineral compounds, with the aim of understanding the influence of nickel sulfide as an additive during the hydrotreatment of this mineral matrix from the Tarfaya (Morocco) oil shale under dynamic conditions. The techniques adopted in this study are true thermogravimetry (Red-Croft), calorimetry (DCE) coupled in Red-Croft, X-ray diffraction and dispersive X-ray diffraction coupled by scanning electron microscope. Carbonate decomposition activity was observed during this nickel sulfide addition, preventing in situ decomposition of NiSO<sub>4</sub> · 6H<sub>2</sub>O in the presence of hydrogen, and increasing conversion of calcite, dolomite, kaolinite and quartz.

Copy Right, IJAR, 2024,. All rights reserved.

#### Introduction:-

The hydrogenation of CO activated with 50% Co 50% Ni as catalyst depends on the oxidized support. The activity in the presence of MgO, PbO and ZnO oxides becomes lower for the metal Co-Ni, on the contrary it becomes higher for TiO<sub>2</sub> and MnO<sub>2</sub>. The adsorption of monoxidized carbon and hydrogen becomes weaker as the electronegativity of the oxide support increases ((T. Ishihara at al :1991), and similarly weakens as the density of the support alloy increases. Hydrogen is of prime importance for this catalyzed system, as the rate of H<sub>2</sub> exchange → D<sub>2</sub> correlates well with the rate of CO hydrogenation. Nickel from shale during degradation is maintained in the oil, from shale deposits in Queensland, Australia (266), under Fisher test conditions. During degradation, the oil and water released are chemically analyzed, and the various trace elements are compared. There are many similarities in the appearance of these elements, although their concentration varies. There is a strong correlation between mineralogical and geological results: arsenic, nickel, cobalt and iron are retained in the oil, while selenium, chlorine and bromine are retained in the free water. We found it interesting to examine the mineral matrix of the Tarfaya shale during dynamic hydrolysis in the presence of sulfide.

#### 1/ Literature Review:-

Nickel catalysis in the presence of molybdenum NiMo/γ--- Al<sub>2</sub>O<sub>3</sub> was carried out for three tars from three Australian coals (P.F. Neson: 1988) in pyrolysis and flash hydrotreating. Analyses by gas chromatography-mass spectrometry, using sulfur alloys and commercial sulfite as product, show that the majority of the oil's compounds are substituents of cyclohexane, tetralin alkylbenzene and n-alkane (C6 to C36). Apart from an increase in product volatility, the compositions detected by chromatography did not change with temperature variation. At higher temperatures, some

Corresponding Author:- Abdeljabbar Attaoui

Address:- Department of Chemistry, Faculty of Sciences Ben m'sik Casablanca, University Hassan II (Morocco).

aromatic products are detected. Nickel in the form of the powdered compound  $\text{LaNi}_5$  absorbs hydrogen, and the reaction is isothermal and isobaric (**Y. Tung et al: 1986**). The data are interpreted by a model with three constraints in series: gas-liquid transfer resistance, liquid-solid transfer resistance and reaction resistance. For strong agitation, the conversion of  $\text{LaNi}_5$  to metal hydride is at most 90% for a duration of at least one minute. Nickel forms mixed complexes with  $\gamma$  and  $\beta$ pycoline. This synthesis, characterized by thermogravimetry (**N. Hurduc and L. Odochian: 1983**) under dynamic temperature conditions, confirms the formation of these complexes. The reaction of graphite in the presence of hydrogen  $\text{C}/\text{H}_2$  to produce methane ( $\text{CH}_4$ ) was carried out using nickel as the catalyst.

The overall reaction takes place in a number of stages, starting with carbon dissolution at the monolayer interface, Ni diffusion and carbon reaction by hydrogen chemisorption at the Ni/gas interface. The last stage is the one that delimits the reaction rate. An order has been suggested and the activity is higher than when using Pt (**P.J. Goethel and R.T. Yang: 1987**). Concerning Iron catalysts, which have two electrons less than nickel, as well as NiMo and CoMo catalysts, it has been concluded that alumina or silicate supports are favorable for the thermal degradation of bitumen, Iron sulfate affects the hydrogenolysis of aromatics and commercial catalysts catalyze hydrodesulfurization in addition to hydrogenolysis (**S. Yokoyama et al: 1993**). Hydrocarbon production is achieved by the reaction between  $12\text{CO}$  and  $13\text{CO}$  in the presence of hydrogen using  $\text{Ni}/\text{Al}_2\text{O}_3$  as catalyst between temperatures  $225$  and  $275^\circ\text{C}$  (**D.M. Stockwell and C.O. Bennett; 1988**). Experiments were carried out in a low-conversion microreactor. N-alkanes and olifins are produced, methane selectivity varies between 40 and 91% and traces of acetaldehydes were detected.  $13\text{C}$  enriches  $\text{C}_3$  better than methane and ethane. Gasification of graphite with  $\text{H}_2\text{O}$  vapor, dry  $\text{H}_2$  and dry  $\text{O}_2$  was carried out in the presence of  $\text{Ni}/\text{K}$  as catalyst. In the presence of  $\text{H}_2\text{O}$  vapor, carbon consumption takes place between  $550$  and  $1100^\circ\text{C}$  and is catalyzed by an edge recession mode with activation energies of  $30.8 \pm 0.9$  kcal/mol. The values are those obtained from the kinetic study of graphite gasification by steam and coal. For dry hydrogen (**J. Carrazza et al: 1988**) the activation energy obtained is  $30 \pm 2$  kcal/mol, the catalyst deactivates at  $1000^\circ\text{C}$  but can be regenerated by treating the sample with steam at  $600^\circ\text{C}$ . In the case of dry  $\text{O}_2$ , gasification can also be achieved by recession at the edge, like dry  $\text{H}_2$ . The activation energy is  $25 \pm 2$  kcal/mol. These results show that the catalytic properties for the  $\text{Ni}/\text{K}$  mixture are superior to those for Ni and K alone. The rate of  $\text{NiO}-\text{MoO}_3/\text{Al}_2\text{O}_3$ -catalyzed hydrogenation at  $340^\circ\text{C}$  under 70 bars of hydrogen is often higher for phenols and their substituents and for benzenes and their substituents (**C. Aubbet et al: 1988**). It may be related to delocalized  $\pi$ -electrons between series of organic compounds. The hydrogenation rates of phenol ortho and para substituents are similar and are lower than those of phenol alone. Hydrogen chemisorption by supported metal catalysts such as 10%  $\text{Fe}/\text{Al}_2\text{O}_3$ , 10%  $\text{Fe}/\text{SiO}_2$ , 10%  $\text{Ni}/\text{Al}_2\text{O}_3$  and 5%  $\text{Ru}/\text{TiO}_2$  is carried out at  $473\text{K}$  and  $773\text{K}$  (**D.M. Stockwell et al: 1988**), using temperature-programmed desorption. Adsorption is weak at  $300\text{K}$ . Catalysis of graphite hydrogenation by Pt, Ni and Ru takes place in such a way that the metal particles form a tunnel in the direction of the graphite, which is parallel to the ground plane (**P.J. Goethel and R.T. Young: 1988**). The linear speed of tunnel formation depends on sample size. The sequences of the phenomenon are the breaking of the C-C bonds, the dissolution of the carbon in the metal loaded with the carbon-metal interface band, the diffusion of the carbon into the metal and the reaction between C and H at the metal surface, with the last step delimiting the reaction. The preparation of  $\text{SiO}_2$ -supported Ni catalyst (**B. Mile et al: 1988**) shows the formation of two distinct types of NiO which reduce at different temperatures under programmed temperature reduction (TPR) conditions. Examination of the pore effects and experiments distinguishes between small-pore (9nm) and large-pore (15 - 30nm) oxide concentrations, with the most reducible oxide localized to the small pores and the least reducible to the large pores. We also note that for the most reducible oxide, there is little interaction with the silicate. TPR shows that oxidized nickel and crystalline nickel are immobilized in the silicate pores at temperatures above  $600^\circ\text{C}$ . Nickel's role is to activate selective hydrogenation (**R.G. Oliver and P.B. Wells: 1972**) for 1,2 and 1,3 butadiene. The formation of coke by  $\text{Ni}/\text{Al}_2\text{O}_3$  catalyzed hydrogenolysis of cyclopentane has been studied in a temperature range of  $300 - 500^\circ\text{C}$ . A similar exchange for activation energy is obtained by catalysis with surface-catalyzed carbon filaments (**R.G. Oliver and P.B. Wells: 1990**). Hydrogenolysis and hydrogenation activities depend on the nature of the deposited carbon, with nickel accounting for a significant proportion of this activity. Embrittlement of nickel by hydrogen in solution is generally accompanied by a change in the mode of fracture (**A. Kimura and H.K. Birnbaum: 1988**). Concerning palladium, which has the same chemical properties as nickel, determination of the variation in hydrogen diffusibility in Pd-Ag membranes as a function of temperature between  $280$  and  $333\text{K}$  and for an Ag concentration of between 0 and 30% was carried out by McLellan (**T. Ishikawa and R.B. McLellan: 1986**). For a given temperature, hydrogen diffusibility shows a small initial increase with increasing Ag concentration. For ruthenium, which belongs to the cobalt group with one electron less than nickel, catalytic hydrogenation of CO by  $\text{Rh}/\text{TiO}_2$ ,  $\text{Rh}/\text{Al}_2\text{O}_3$  and  $\text{Rh}/\text{SiO}_2$  was carried out at a temperature of  $673^\circ\text{K}$ . The highest activity is achieved by  $\text{Rh}/\text{TiO}_2$ . CO reactivity by  $\text{Rh}/\text{Al}_2\text{O}_3$  is proportionally limited by an intermediate reaction. Reactivity by  $\text{Rh}/\text{SiO}_2$  is lower due to an intermediate reaction, which shows us that CO

activation is greatly influenced by the support used (I. Mochida et al: 1988). The gasification of coal in the presence of copper, which has one electron more than nickel, has been compared with that using vanadium oxide and it has been shown that samples containing copper are reactive at high temperatures (**C.M. Castilla et al: 1989**). Co/Al<sub>2</sub>O<sub>3</sub>-catalyzed CO hydrogenation using the surface temperature programmed reaction (TPSR) technique showed the appearance of two peaks corresponding to methane formation at 15% Co/Al<sub>2</sub>O<sub>3</sub> (**W.H. Lee and C.H. Bartholomen; 1989**). The non-methane peaks form at a Co/Al<sub>2</sub>O<sub>3</sub> content of at least 1% and at 1023K. Spectral GSTR of hydrogen with carbon deposited by CO dissociation at 523K shows that the amount of active carbon increases with metal loading. Hydrogen transport during plastic deformation was studied by secondary ion mass spectroscopy in type 304 stainless steels and nickel. Deuterium profiles for samples electrochemically charged during deformation and for undeformed samples were measured.

## 2/ Experimental study:

We will first look at nickel sulphate pentahydrate NiSO<sub>4</sub> · 6H<sub>2</sub>O and its behavior towards hydrogen.

### 2.1; Characterization of nickel sulphate hexahydrate NiSO<sub>4</sub> · 6H<sub>2</sub>O.

The β form of nickel sulphate hexahydrate is green, monoclinic and stable at elevated temperature (**Phyllipps and Copper: 1826**). The water molecules are grouped octahedrally around the nickel ions. The blue-colored α-form is easily obtained in fine crystals by evaporation of an acid sulfate solution at ordinary temperature, or of a neutral solution between approx. 31 and 53°C. Above this temperature and up to around 70°C, the form is obtained. However, the latter can be obtained at ordinary temperature by initiating crystallization with monoclinic crystals of cobalt or iron sulfate (De. Boisbandran C.R: 1868) or by electrolysis between nickel electrodes (**Tanzov. J: 1924**). It is then metastable and the green crystals gradually become opaque and bluish, giving back the -quadratic variety. The transition point is 53.3°C (**Steele and Johnson: 1904**).

### 2.2: Thermal degradation of NiSO<sub>4</sub> · 6H<sub>2</sub>O under hydrogen.

The reaction conditions are the dynamic regime 21°C/min in a hydrogen flow. The thermogram given by the Red-Croft thermobalance (**A. Attaoui et al: 2022**)

The degradation of NiSO<sub>4</sub> · 6H<sub>2</sub>O under hydrogen from ambient to 940°C was followed in three distinct stages (Fig1):

- Dehydration, which takes place between ambient and 150°C, according to the reaction:



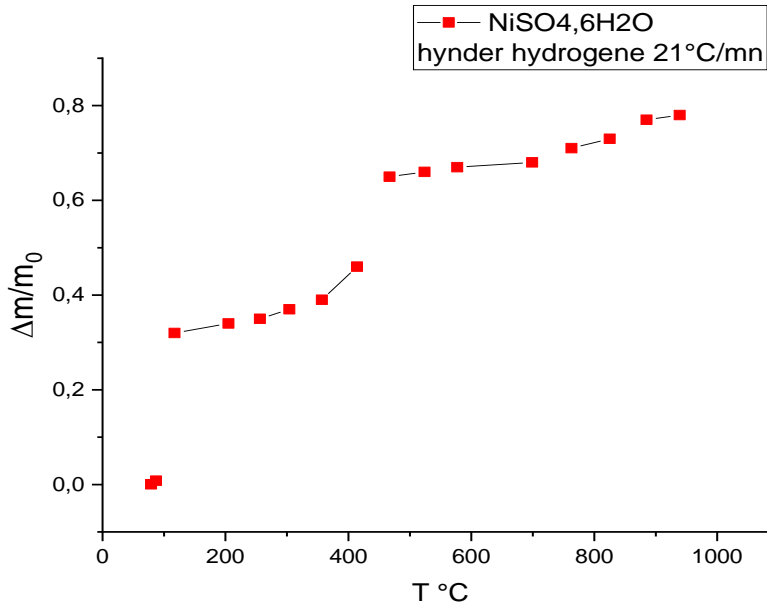


Fig 1:- Thermogram of the decomposition of NiSO<sub>4</sub>, 6H<sub>2</sub>O under hydrogen in the dynamic regime.

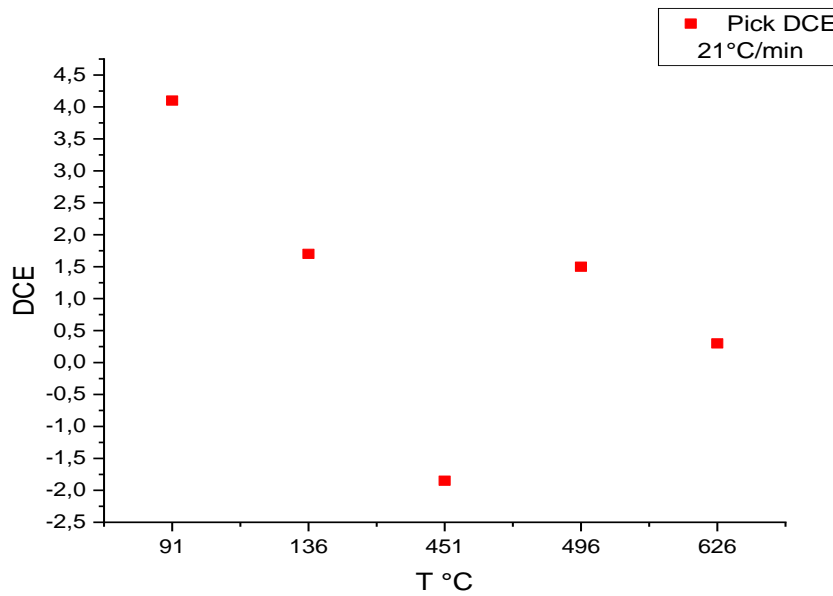
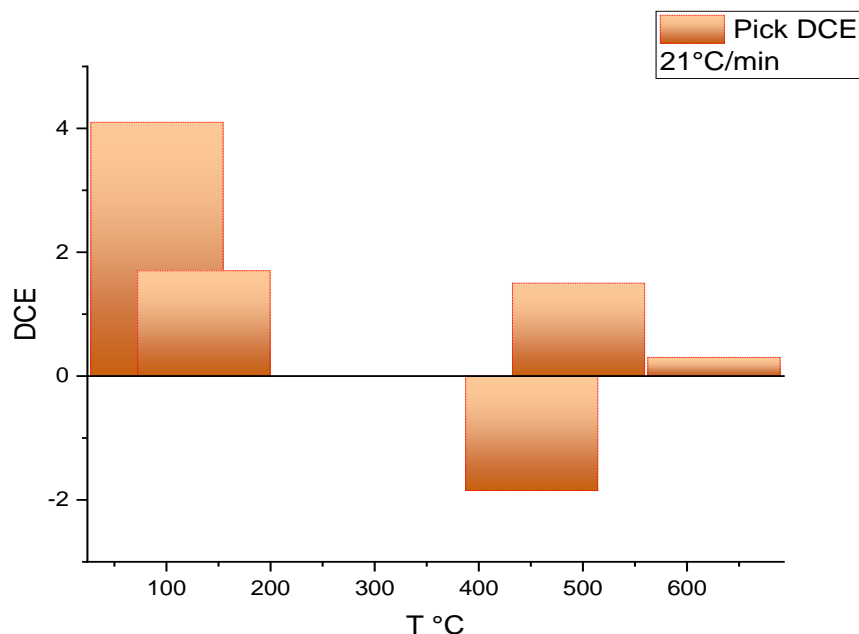


Fig 2:- Maximum temperature of the DCA peak of the decomposition of NiSO<sub>4</sub>, 6H<sub>2</sub>O under hydrogen in the dynamic regime.



**Fig 3:-** Maximum temperature of the DCA peak of NiSO<sub>4</sub>, 6H<sub>2</sub>O decomposition under hydrogen in the dynamic regime as a histogram.

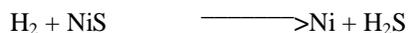
We observe two DCA peaks (Figures 2 and 3), both endothermic, which shows us that this reaction is carried out in two sub-steps, one at 91°C and the second at 136°C.

- Next we have the decomposition of NiSO<sub>4</sub> according to the reaction:



This reaction occurs in two distinct sub-steps with two DCA peaks, due to the dissymmetry of the SO<sub>2</sub>-4 ion. The first DCA peak is exothermic and occurs at a temperature of 451°C, while the second endothermic peak occurs at 496°C.

- Finally, we have the hydrodesulphurisation of NiS according to the reactio:



It is an endothermic reaction (DCA) and starts at 540°C and ends at 940°C. The maximum heat exchange occurs at 626°C.

### 2.3: Physical state of NiS<sub>1-x</sub> (0 ≤ x ≤ 1) under hydrogen

The compound NiSO<sub>4</sub>, 6H<sub>2</sub>O (photo 1, Fig 4) was degraded under ambient hydrogen up to 750°C, this temperature corresponds to a loss fraction of the first product of x = 0.28. SEM photo 1 shows

NiSO<sub>4</sub>, 6H<sub>2</sub>O in its crude state. Photo 2 (Fig 5) shows NiS 0.72 obtained by decomposition of the first product under hydrogen at 750°C.

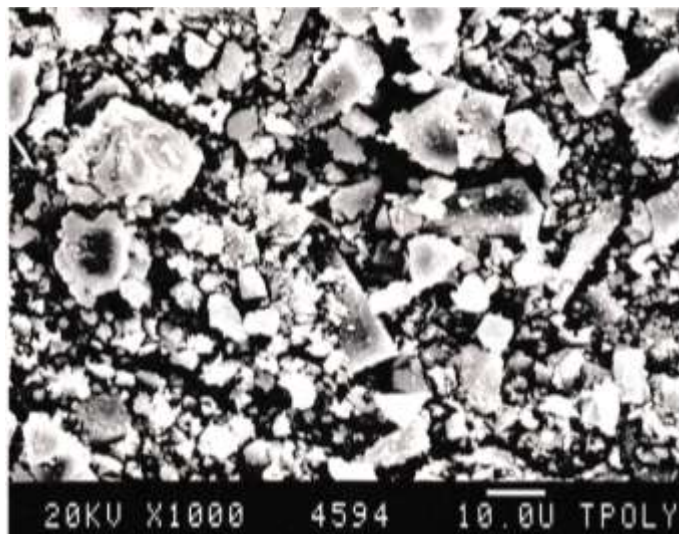


Fig 4:- Photo of raw  $\text{NiSO}_4 \cdot 6\text{H}_2\text{O}$ .

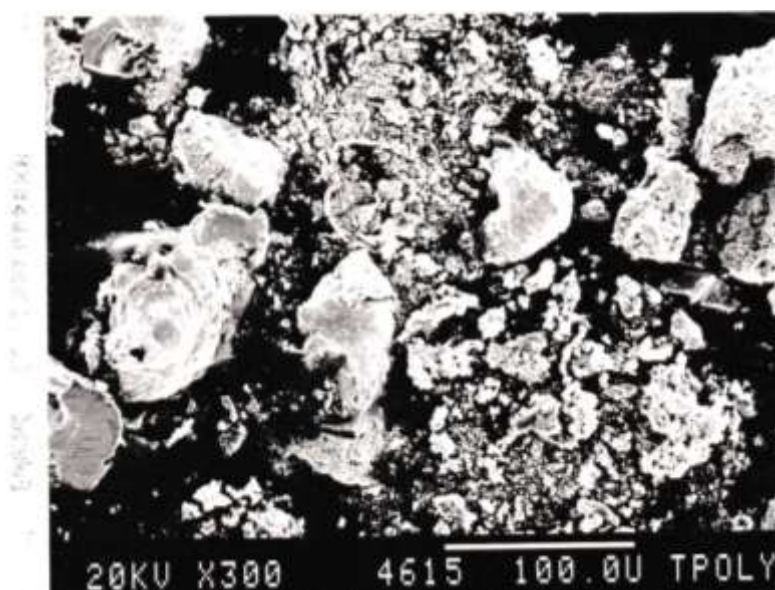
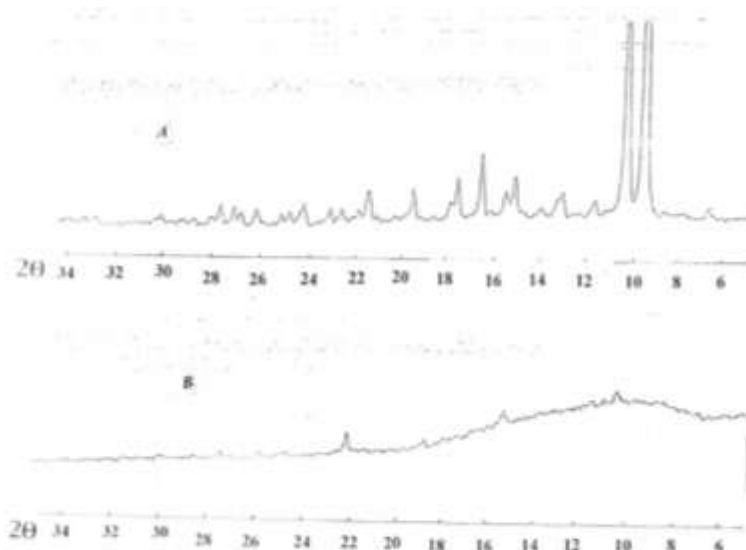


Fig 5:- Photo of  $\text{NiS}_{1-x}$  ( $0 \leq x \leq 1$ ) under  $\text{H}_2$

The two photos above show that after hydrotreatment, the  $\text{NiO}$  0.72 obtained is three times the size of the initial sample. The previous study on the hydrotreatment of hydrated nickel sulphate was necessary, as this compound will be associated with shales in order to understand its role in shale reactivity.

### 3/ X-ray diffraction study

The X-ray diffraction study was carried out on the crude  $\text{NiSO}_4 \cdot 6\text{H}_2\text{O}$  sample and on that hydrotreated up to  $750^\circ\text{C}$  (Figure 6 A, B). At this temperature the sample is in the form:  $\text{NiS}_{1-x}$  ( $0 \leq x \leq 1$ ).



**Fig 6:-** RX diffraction:A raw  $\text{NiSO}_4 \cdot 6\text{H}_2\text{O}$   
 $\text{BNiS}_{1-x}(0 \leq x \leq 1)$  under  $\text{H}_2$  till  $750^\circ\text{C}$ .

#### 4/ Calorimetric study of the decomposition of oil shale carbonates under hydrogen in the presence of $\text{NiSO}_4 \cdot 6\text{H}_2\text{O}$

This calorimetric study was carried out for the five oil shale samples and for three mass fractions of  $\text{NiSO}_4 \cdot 6\text{H}_2\text{O}$ . The peaks detected were those of dehydration and those of carbonate decomposition. The following table shows the temperatures at which the various carbonate decomposition peaks appear.

**Table 1:-** Calorimetric study.

| Samples | Masse fraction of $\text{NiSO}_4 \cdot 6\text{H}_2\text{O}$ |   |  | Oil shale samples alone under $\text{H}_2$            |
|---------|---|---|--|---|
|         | $x=3,3\%$   | $x=5,3\%$   | $x=6,7\%$  |   |
|         | Carbonate decomposition<br>Tpick ( $^\circ\text{C}$ )       | Carbonate decomposition<br>Tpick ( $^\circ\text{C}$ ) | Carbonate decomposition<br>T pick ( $^\circ\text{C}$ ) | Carbonate decomposition<br>Tpick ( $^\circ\text{C}$ ) |
| Z0      | 709   | 696   | 707  | 701   |
| Z1      | 699   | 693   | 687  | 692   |
| Z2      | 692   | 685   | 688  | 689   |
| Z3      | 680   | 685   | 683  | 668   |
| Z4      | 680   | 698   | 674  | 677   |

By comparing these temperatures with those of the decomposition of the carbonates when the samples are alone, and by putting a negative sign when there is activation and a positive sign when there is deactivation, the difference in temperature obtained is equal to:

$$\sum \Delta T / \sum i = 5^\circ\text{C}$$

This is a positive value and corresponds to deactivation of the decomposition of oil shale carbonates in the presence of hydrated nickel sulphate. This deactivation, converted into energy using the heat capacity of the apparatus ( $C_p=0.62 \text{ j/g}^\circ\text{K}$ ) (Awbery; 1938) is of the order of:  $\Delta E = 3,1 \text{ J/g}$ .

### 5/ Thermogravimetric study

This study was followed by the Red-Croft thermobalance in dynamic regime (21°C/min) under ambient hydrogen up to 750°C. Figure 7 shows the thermograms without addition of NiSO<sub>4</sub>, 6H<sub>2</sub>O (A. Attaoui : 2023), figure 8 with addition of NiSO<sub>4</sub>, 6H<sub>2</sub>O.

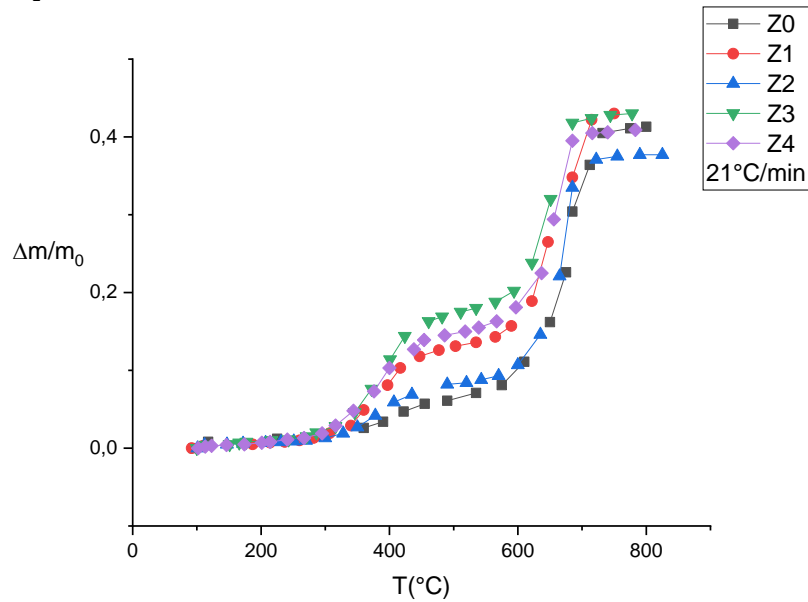


Fig 7:- Thermograms of different layers under hydrogen.

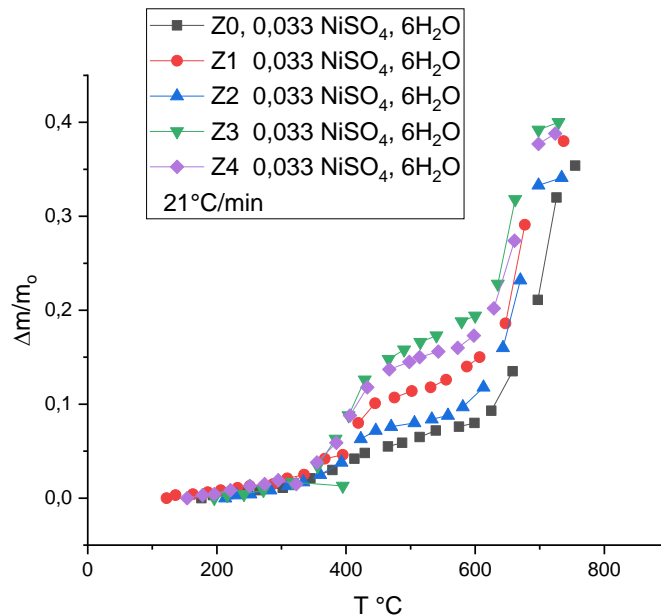


Fig 8:- Thermograms of different layers with addition of NiSO<sub>4</sub>, 6H<sub>2</sub>O under hydrogen.

### 6/ Degree of decomposition of desiccated carbonates by NiS<sub>1-x</sub> (0 ≤ x ≤ 1) during hydrotreatment

The thermogravimetric study was followed, and the degree of progress of the degradation of oil shale carbonates under hydrogen in the presence of NiS<sub>1-x</sub> (0 ≤ x ≤ 1) was compared for the six samples, with that in the absence of nickel sulphate (figure 9). We noted strong activity at the start of degradation, which was remarkable for samples Z1, Z3 and Z4. This shows the activating effect of NiSO<sub>4</sub>, which decomposes at a temperature slightly lower than that of the decomposition of the carbonates alone. Unfortunately, the deactivating effect of NiS<sub>1-x</sub> (0 ≤ x ≤ 1), previously noted by DCA, is clearly seen from the temperature of 650°C and higher. This phenomenon can be explained by observing

the DCA curve (figure 2) for hydrotreated hydrated nickel sulphate, which shows a more intense exothermic reaction at 451°C followed by an endothermic reaction at 496°C. The energy released by the exothermic effect activates the degradation of the carbonates at their onset. It should be noted that these Tarfaya layers were formed during the Upper Cretaceous in warm climates (A. Attaoui et al: 2022).

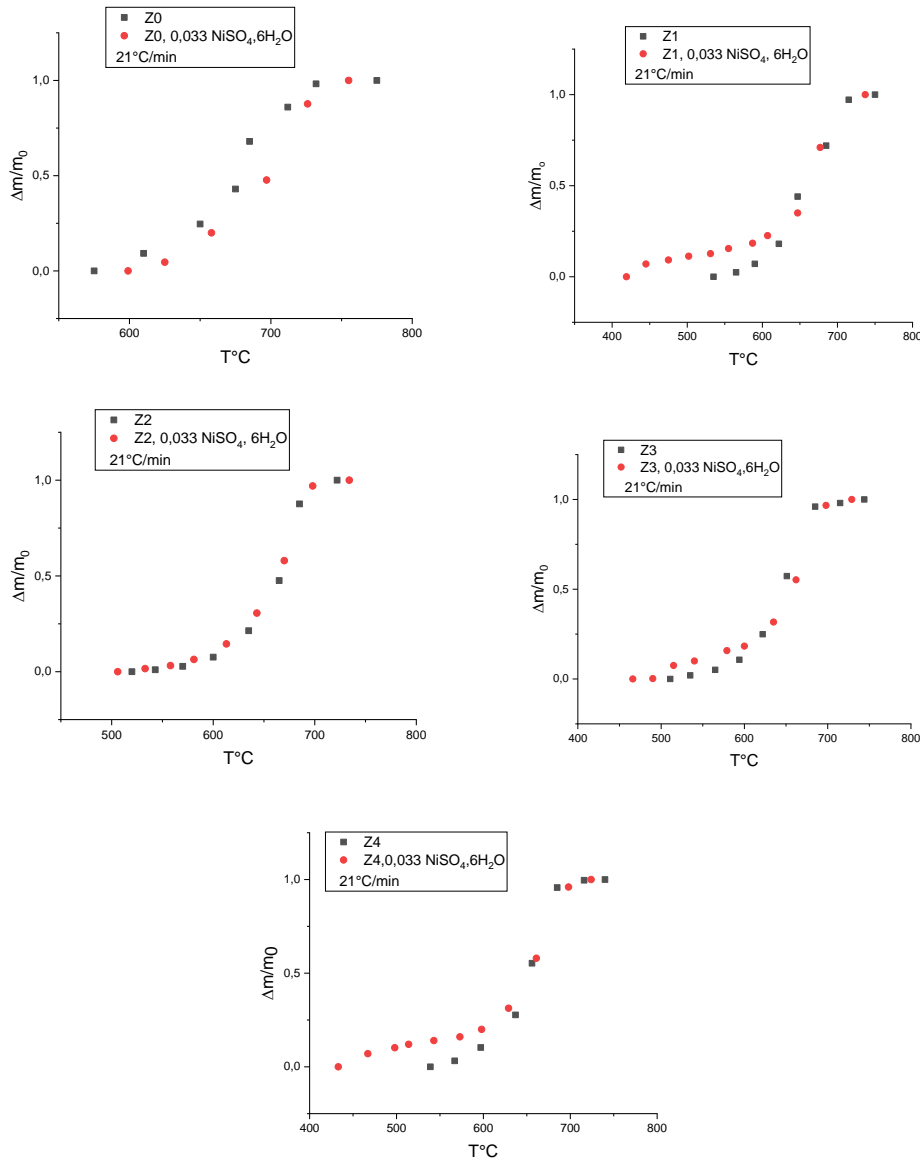
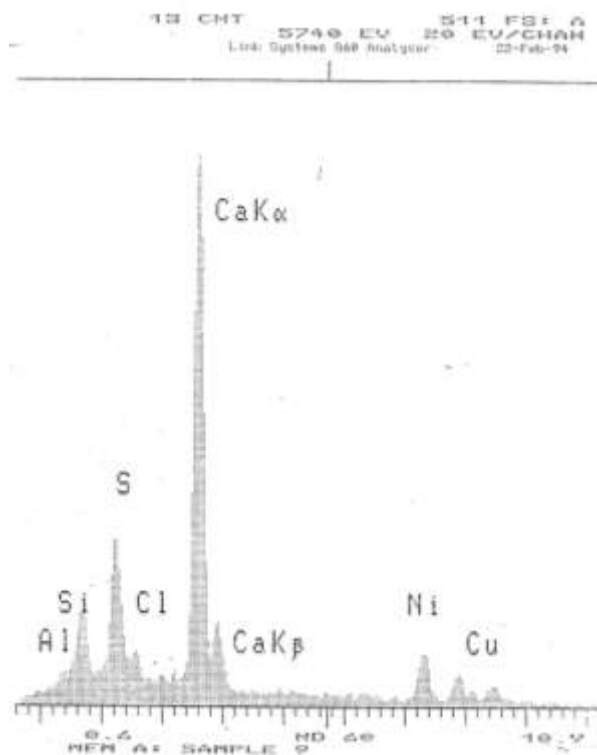


Fig 9:- Thermograms in  $\alpha=f(T)$  of carbonates for the five-oil shale sample.

- alone
- in presence of  $NiS_{1-x}(0 \leq x \leq 1)$ prevenantof the decomposition for  $NiSO_4, 6H_2O$  under hydrogen

**7/ Conversion of the various carbonate constituents during hydrolysis in the presence of  $NiSO_4, 6H_2O$ .**

Dispersive X-ray diffraction analysis was carried out for sample Z3 hydrotreated alone and for sample Z3 hydrotreated in the presence of hydrated nickel sulphate  $NiSO_4, 6H_2O$  (Fig 10).



**Fig 10:-** Spectre RXD for Z3 hydrotreating in presence of  $\text{NiSO}_4 \cdot 6\text{H}_2\text{O}$ .

The elementstobe analysed are calcium $\alpha$ , calcium $\beta$ , silicon, chlorineandsulphur.

The following table represents the size of each peak in centimetres and the percentage of presence of each element.

The dimension values in the table are relative to an A4 page of the record, while the figure is a collapsed copy

**Table 2:-** Percentage of chemical elements in the Tarfaya oil shale.

| Composition           | Z3 hydrotreated till 750°C | Z3,0,033 $\text{NiSO}_4 \cdot 6\text{H}_2\text{O}$ hydrotreated till 750°C |
|-----------------------|----------------------------|--|
| Silicon(cm)           | 1,75                       | 2,5  |
| Silicon (%)           | 9,4                        | 9,0  |
| Sulphur(cm)           | 1,2                        | 5,1  |
| Sulphur (%)           | 6,4                        | 18,3   |
| Chlorine(cm)          | 0,9                        | 1,7  |
| Chlorine (%)          | 4,8                        | 6,1  |
| Calcium $\alpha$ (cm) | 12,9                       | 16,6   |
| Calcium $\alpha$ (%)  | 69                         | 59,7   |
| Calcium $\beta$ (cm)  | 1,95                       | 2,5  |
| Calcium $\beta$ (%)   | 10,4                       | 9,0  |

Sulphur is part of  $\text{NiSO}_4 \cdot 6\text{H}_2\text{O}$  and is also part of the composition of pyrite, which is a constituent of oil shale. It is difficult to discern the type of sulphur to be followed; the following table shows the increase in conversion of the constituents of the mineral matrix of oil shale in the presence of  $\text{NiSO}_4 \cdot 6\text{H}_2\text{O}$ .

**Table 3:-** Increased or reduction conversion of oil shale constituents in presence of  $\text{NiS}_{1-x} (0 \leq x \leq 1)$ .

| Elements             | Constituents       | Percentage of conversion Improvement       | Percentage reduction in conversion         |
|----------------------|--------------------|--|--|
| Silicon              | Quartz, Kaolinite  | $(100 - (9/9,4 \times 100)) \% = 4,3\%$    | -----                                      |
| Chlorine             | Chlorine compounds | -----                                      | $(100 - (4,8/6,1 \times 100)) \% = 21,3\%$ |
| Calcium <sub>q</sub> | Calcite, Dolomite  | $(100 - (59,7/69 \times 100)) \% = 13,5\%$ | -----                                      |
| Calcium <sub>p</sub> | Calcite, Dolomite  | $(100 - (9/10,4 \times 100)) \% = 13,5\%$  | -----                                      |

The presence of  $\text{NiS}_{1-x} (0 \leq x \leq 1)$  during the hydrotreatment of the mineral matrix in the dynamic regime leads to three selective possibilities depending on the constituents of this mineral matrix:

We have:

- a 4.3% increase in conversion of Quartz, Kaolinite,
- a 13.5% increase in the conversion of calcite and dolomite,
- and a 21.3% decrease in the conversion of chlorinated compounds.

### Conclusion:-

The element Nickel forming part of the nickel sulphate pentahydrate  $\text{NiSO}_4 \cdot 6\text{H}_2\text{O}$  decomposing into nickel sulphide  $\text{NiS}_{1-x} (0 \leq x \leq 1)$  was the subject of an addition in mass fraction during the hydrolysis reaction in dynamic regime ( $21^\circ\text{C}/\text{min}$ ) of the various oil shale layers of the Tarfaya deposit (Morocco).

Firstly, we monitored the decomposition of nickel sulphate pentahydrate  $\text{NiSO}_4 \cdot 6\text{H}_2\text{O}$  under hydrogen in a dynamic regime under the same conditions, which takes place in three stages using thermogravimetry and five stages using calorimetric analysis (DCE), which are clearly distinguishable. Four are endothermic and one is exothermic at  $451^\circ\text{C}$ .

The product of this decomposition under hydrogen  $\text{NiS}_{1-x} (0 \leq x \leq 1)$ , which in turn degrades between  $540^\circ\text{C}$  and  $940^\circ\text{C}$ , the range where we have hydrotreating of the mineral matrix of oil shale, was added as an initial mass fraction during this hydrolysis of the different layers of Tarfaya oil shale. Several results were obtained depending on the analysis technique used:

In calorimetry (DCE), we carried out the hydrotreatment reaction for the five samples at three mass fractions of  $\text{NiSO}_4 \cdot 6\text{H}_2\text{O}$ : 0.033, 0.053 and 0.067, and we also carried out the tests for the samples alone. We then calculated the average of the different tests and the difference with the average of the tests alone. This difference is positive at  $5^\circ\text{C}$ , giving a deactivation energy of around 3.1 j/g.

The degree of progress in thermogravimetric degradation of oil shale carbonates under hydrogen in the presence of  $\text{NiS}_{1-x} (0 \leq x \leq 1)$  was compared for the six samples with that in the absence of nickel sulphate (Figure 9). We noted a high level of activity at the start of degradation, which is remarkable for samples Z1, Z3 and Z4. This shows the activating effect of  $\text{NiSO}_4$ , which decomposes at a temperature slightly lower than that of the decomposition of the carbonates alone, while the deactivating effect of  $\text{NiS}_{1-x} (0 \leq x \leq 1)$  noted previously by DCA is clearly seen from the temperature of  $650^\circ\text{C}$  and higher. This phenomenon can be explained by observing the DCA curve (figure 2) for hydrotreated hydrated nickel sulphate, which shows a more intense exothermic reaction at  $451^\circ\text{C}$  followed by an endothermic reaction at  $496^\circ\text{C}$ . The energy released by the exothermic effect activates the degradation of the carbonates at their onset. These Tarfaya layers were formed during the Upper Cretaceous in warm climates.

The hydrotreatment of the mineral matrix in the dynamic regime in the presence of  $\text{NiS}_{1-x} (0 \leq x \leq 1)$  leads to three selective possibilities depending on the constituents of this mineral matrix:

- These three selective possibilities are;
- first 4.3% increase in the conversion of Quartz and Kaolinite,

second 13.5% increase in the conversion of Calcite and Dolomite, and third 21.3% decrease in the conversion of chlorinated compounds.

### Reference:-

- [1] T. Ishihara and all Journal of catalysis 1991. Vol. 130. 202-211.
- [2] P.F. Nelson Fuel 1988. Vol. 67. January 86.
- [3] Y. Tung et al. AICHE. Journal 1986. Vol. 32 N°11. Novem. 1821.
- [4] N. Hurduc and L. Odochian. Journal of thermal. Analysis 1983. Vol.28. 11-16
- [5] P.J. Goethel and R.T. Yang. Journal of catalysis. 1987. 108. 356-363.
- [6] S. Yokoyama et al. Fuel. 1993. Vol. 72. N°4. 573.
- [7] D.M. Stockwell and C.O. Bennett. Journal of Catalysis 1988. 110-354.
- [8] J. Carrazza and all. Journal of Catalysis 1988. 110. 74-81.
- [9] C. Aubert and all. Journal of Catalysis 1988. Vol. 112. 12-20.
- [10] D.M. Stockwell et al. Journal of Catalysis 1988. 113. 317-324.
- [11] P.J. Goethel and R.T. Youg. Journal of Catalysis. 1988. 114. 46-52.
- [12] B. Mile et al. Journal of Catalysis. 1988. 114. 217-229.
- [13] R.G. Oliver and P.B. Wells Proceeding of fifth international Congress. On Catalysis. Miami Beach 1972. August 20-26.
- [14] D. Duprez and all Journal of Catalysis 1990. 124. 324-335.
- [15] A. Kimura and H.K. Birnbaum. Acta. Metall. 1988. Vol. 36. N°3. 757.
- [16] T. Ishikawa and R.B. Mclellan. Acta. Metall 1986. Vol. 34. N°9.1832.
- [17] I. Mochida and all. Journal of Catalysis. 1988. Vol. 110. 159.
- [18] C.M. Castilla and all. Fuel. 1989. Vol 68. August 968.
- [19] W.H. Lee and C.H. Bartholomen. Journal of Catalysis. 1989. Vol. 120. 256
- [20] Phylipps and Copper. Ann. Physik 6-194-1826.
- [21] De. Boisbandran C.R. 66-497- 1868.
- [22] Tanzov. J. Soc. Phys. Chim. Russe. 55-335-1924.
- [23] Steele and johnson. J. Chem. Soc. (Trans) 85-116. 1904.
- [24] A. Attaoui et al, Mineral matter hydrolysis of Tarfaya oil shale and influence of sedimentation edge, Oil Shale.2022 Vol, No.4, pp.290-307.doi:<https://doi.org/10.3176/oil.2022.4.04>
- [25] Awbery. Phil. Mag. 26. 776. 1938.
- [26] A. Attaoui Activation energies by Coast-Redfern approximations of the mineral matte hydrolysis for the Tarfaya oil shale (Morocco). Modeling to obtain these energies for the different layers in non-isothermal.Int.J.Adv.Res DOI:10.21474/IJAR01/17280, July2023,10(07), 712-724
- [27] Ahmed Malal, Doha Lahmadi and AbdeljabbarAttaoui, "Type of burial and adaptation of the geological ages with the sedimentation of the organic matter for the differentlayersfor the Tarfaya's oil shale deposit (Morocco)", Int.J.Adv.Res.10(04),372-382, April2022, DOI:10.21474/IJAR01/14557.